Supplemental Experimental Procedures Chen H, et al.

DEPTOR Suppresses Lipogenesis and Ameliorates Hepatic Steatosis and Acute-on-Chronic Liver Injury in Alcoholic Liver Disease

Short Title—Defective Signaling of SIRT1 and DEPTOR Contributes to Alcoholic Fatty Liver in Mice and Humans

Hanqing Chen[1,2], Feng Shen[1,2,3], Alex Sherban[4], Allison Nocon[4], Yu Li[4,5], Hua Wang[6], Ming-Jiang Xu[6], Xianliang Rui[4], Jinyan Han[4], Bingbing Jiang[4], Donghwan Lee[1,2], Na Li[1,2,7], Farnaz Keyhani-Nejad[1,2], Jian-gao Fan[3], Feng Liu[2], Amrita Kamat[8], Nicolas Musi[2,8], Leonard Guarente[9], Pal Pacher[6], Bin Gao[6], Mengwei Zang[1,2,8]*

A Mouse Model of Chronic-Plus-Binge Ethanol Feeding and Rapamycin Treatment

The experimental mouse model of alcoholic liver disease (ALD) was developed by Bin Gao's group as recently described (1, 2). Hepatocyte-specific SIRT1 knockout (Sirt1 LKO) mice were achieved by crossing albumin-Cre recombinase transgenic mice with floxed SIRT1$^{\Delta ex4}$ mice containing the deleted SIRT1 allele with floxed exon 4 (3). Mice at 14-20 weeks of age were placed on a chronic 5% (v/v) ethanol feeding liquid diet *ad libitum* for 10 days with a single binge of ethanol feeding (5 g/kg). As shown in **Fig. 1S**, C57BL/6 mice were acclimated to the control liquid diet (Bio-Serv, Cat#F1259SP, Frenchtown, NJ, USA) for 5 days prior to the initiation of experiments. The mice were either free fed with a Lieber-DeCarli liquid ethanol diet (Bio-Serv, Cat#F1258SP, Frenchtown, NJ, USA) or pair-fed with the same volume of an isocaloric control diet. After 10 days of ethanol administration or control diet, ethanol-fed mice (n = 10-15) and pair-fed mice (n = 7-10) were gavaged with a single dose of ethanol (5 g/kg body weight) or isocaloric dextrin-maltose, respectively, in the early morning of Day 11 and sacrificed 9 hours later. All mice were weighed at the beginning of the feeding period and daily thereafter until sacrifice. When mice were euthanized, one portion of liver tissue was rapidly taken, freshly frozen in liquid nitrogen, and stored at -80°C until needed for immunoblotting analysis. The remaining liver tissue was fixed for histological and immunohistochemical analysis. All mice were housed in a temperature-controlled environment with a 12-h light/dark cycle. All animal experiments were approved by the Institutional Animal Care and Use Committee (IACUC) at the University of Texas Health Science Center at San Antonio (UTHSCSA).

To determine the effect of rapamycin administration on the development of ALD, chronic-plus-binge ethanol-fed mice were given daily intraperitoneal injections of either vehicle control or rapamycin at a dose of 1 mg/kg/day as described previously (4-6). Both groups of the mice were maintained on the ethanol feeding for 10 days, followed by a single binge of ethanol (5 g/kg). Mice were sacrificed under isoflurane anesthesia 9 h after gavage. Body weight and food intake were monitored daily during the 10 days of ethanol administration. Rapamycin was obtained from LC Laboratories (Woburn, Massachusetts, USA), dissolved in 2 ml of 100% dimethyl sulfoxide (DMSO) to make a stock solution of rapamycin at 20 mg/ml, and stored at -20°C. The rapamycin stock solution for intraperitoneal injections was diluted to 2 mg/ml in phosphate buffered saline (PBS). Each mouse received daily intraperitoneal injections of rapamycin at 1 mg/kg body weight/dose in a total injection volume of 0.3 ml, but control animals received the DMSO vehicle at 0.33% in a total injection volume of 0.3 ml.

Cell Culture and Ethanol Treatment

The alpha mouse liver 12 (AML 12) hepatocytes purchased from American type culture collection (ATCC) were cultured in 1:1 mixture of DMEM (1 g/L D-Glucose) and Ham's F12 medium (Invitrogen) supplemented with 10% fetal bovine serum (FBS, Invitrogen), 40 ng/mL Dexamethasone, 0.005 mg/mL transferrin (Invitrogen), and 1% penicillin/streptomycin (Invitrogen) as described previously (7). Mouse RAW264.7 macrophages (ATCC) were cultured in DMEM (1 g/L D-Glucose) supplemented with 10% FBS and 1% penicillin/streptomycin as described previously (8). The cells were grown and maintained in a humidified atmosphere of 5% CO_2 at 37°C. The cells were incubated in complete medium with 10% FBS in a 100-mm-diameter dish to 70-80% confluence and maintained in culture medium containing 2% FBS overnight. Increasing concentrations of ethanol (25-100 mM) were added to the cultured plate, followed by incubation for an additional 6-24 h.

In Vivo Adenoviral Gene Transfer

The recombinant adenoviral vector expressing human DEPTOR was generated as described previously (9-13). The cDNA clone for human DEPTOR (14) was purchased from Addgene (cat# #21334). The adenoviral vector encoding DEPTOR was constructed using a Gateway pAd/CMV/V5-DEST vector and a ViraPower Adenoviral Expression System (Invitrogen) according to the manufacturer's instructions. Briefly, the DEPTOR cDNA was inserted into the expression plasmid pCMV-SPORT6. The full-length cDNA of DEPTOR with attB-sites was subcloned into a Gateway pDONR™221 vector (Invitrogen) via BP ClonaseTM II enzyme (Invitrogen) to create an entry clone. Subsequently, the DEPTOR expression cassette was subcloned from the entry vectors into the pAd/CMV/V5-DEST expression vector (Invitrogen) using LR-reaction II (Invitrogen). The pAd/CMV/V5-DEST plasmid encoding DEPTOR was linearized by Pac1 endonuclease and the linearized adenoviral vector was subsequently transfected into a mammalian HEK293A package cell line with Lipofectamine 2000 (Invitrogen). Infected cells and cultured media were harvested until 80% of the cells detached from plates, followed by three cycles of freeze/thawing using a 37°C water bath and a liquid nitrogen container to obtain the crude viral lysate as described previously(15).

The adenovirus encoding a dominant negative mutant of S6K1 (DN-S6K1), which contains a mutation of lysine 100 to arginine (K100R) in the ATP binding site of the kinase domain (16-18), was a generous gift from Dr. Jianping Ye (Pennington Biomedical Research Center, Louisiana State University System, LA). For the amplification and purification of high-titer recombinant adenoviruses, large-scale HEK293A cells were infected with viral supernatant and purified by using the Adenovirus Purification Kit (Puresyn, Malvern, PA) as described previously (19-21). Adenovirus-mediated gene transfer in the livers of mice was achieved by a tail vein injection of 100 µl of an adenovirus diluted in saline ($1 \times 10^9 \sim 5 \times 10^9$ pfu) per mouse using a 0.1-ml syringe with a 29.5-gauge needle before the chronic-plus-binge ethanol feeding. Overexpression of hepatic GFP in mice was used as the negative control as described previously (19-21).

Measurement of Plasma Levels of Alanine Aminotransferase (ALT)

Plasma alanine aminotransferase (ALT) concentrations were determined by using an Infinity™ ALT (GPT) Liquid Stable Reagent (Thermo Electron, Melbourne, Australia). Briefly, 3 µl of plasma samples were added to a 96-well plate, and the proper 300 µl of reagent was added to the microplate. The optical density (OD) was determined at 340 nm using Spectramax M5 Microplate Reader (Molecular Devices, CA, USA). The plasma ALT concentrations were calculated as following: ALT (U/L) = $\Delta OD_{340\ nm}$/min × 1746.

Measurement of Hepatic and Plasma Lipid Levels

Hepatic triglyceride and cholesterol concentrations were measured in liver tissues as described previously (3, 19, 21, 22). Briefly, liver tissues (20-30 mg) were homogenized in 1 ml of PBS (pH = 7.4) using a Fisher Scientific™ 125 Homogenizer (Fisher, Cat#08451660) for three cycles, 30 seconds each. The homogenates were transferred to clear glass tubes (BD Vacutainer, NJ, USA). The protein concentrations in the lysates were determined by Protein Assay Dye Reagent (Bio-Rad, USA). Homogenates were mixed with 5 ml of chloroform and methanol (2:1, vol/vol). The mixture was vortexed vigorously to allow separation into two phases in the tubes. The lipid extracts were condensed at the bottom phase by centrifuging at 3,000 rpm for 10 min at 4°C. An aliquot of lipid extracts was incubated with 0.6 ml of 4 mM $MgCl_2$ and 1.5 ml of chloroform for 30 min on ice. The lipid mixture was vortexed and centrifuged at 2,000 rpm for 10 min at 4°C. An aliquot of the organic solvent phase was evaporated under nitrogen gas. Lipid extracts of liver tissues were dissolved in 200 µl of isopropanol with 1% Triton X-100. To assay, 3 µl of triglyceride standard or liver lipid extract was added to a 96-well flat bottom polystyrene plate, and 300 µl of Infinity triglyceride or cholesterol reagents were added to the microplate by using Infinity™ Triglyceride or Cholesterol kits (Fisher Diagnostics, VA, USA) according to manufacturer's instructions. After the plate was incubated for 5 min at room temperature, the optical density was measured at 515 nm using the Spectramax M5 Microplate Reader (Molecular Devices, Sunnyvale, CA, USA). Hepatic triglyceride and total cholesterol levels were normalized to protein concentrations and expressed as µg of lipid/mg of protein (19, 21, 22). Similarly, plasma triglyceride or cholesterol levels were measured using Infinity™ Triglyceride or Cholesterol kits, respectively.

Liver Histological Analysis

When animals were sacrificed, liver tissues were rapidly fixed in phosphate-buffered 10% formalin (Cat#SF100-20) for 24-48 h at room temperature and embedded in paraffin. Paraffin sections (4 µm) were cut and mounted on glass slides. After dehydration, the sections were stained with hematoxylin and eosin as described previously (22-24). To analyze liver lipid infiltration, 5-10 randomly sections were examined, and the unstained vacuoles were visible in the H&E stained liver sections of the mice on the ethanol diet. After mounting, the liver sections were viewed under Nikon Eclipse 80i microscope with 10X and 20X objectives. Staining images were captured and digitalized using a Nikon DS-Fi1 digital camera attached to the Nikon Eclipse 80i microscope.

Immunohistochemistry

Immunohistochemistry of liver tissue sections was performed as described previously (22-25). After deparaffinization and rehydration, 4-µm thick liver sections were incubated with 10 mmol/L citric acid (pH 6.0) and heated in a microwave at 700 W for 2 min with repeated three times to unmask the antigenicity. Upon cooling, liver tissue sections were incubated in 3% hydrogen peroxide solution for 10 min to quench endogenous peroxidase activity. Sections were washed in PBS and 0.1% Tween 20 (PBST) at room temperature for three times, each wash lasting 5 min. To block the nonspecific binding, the liver sections were incubated for 20 min at room temperature with universal IHC blocking buffer from Power Vision+Poly-HRP IHC Detection Systems (Leica, #PY6103) according to manufacture instructions.

For immunohistochemistry staining, the liver sections were placed in a wet box and incubated with the primary antibody in PBST with 1% BSA at 4°C overnight. The following primary antibodies were used: phospho-S6 (Ser235/236) (CST#2211, 1:200), DEPTOR (Millipore#ABS222, 1:150), SREBP-1 (sc#367 K-10, 1:100), and lipin 1 (CST#14906, 1:100). The sections were washed three times in PBST and incubated in post-blocking buffer from Power Vision+Poly-HRP IHC Detection Systems (Leica, #PY6103) for 20 min at room temperature. The liver sections were washed in PBST three times and incubated for 1 h at room temperature with the HRP-conjugated second antibody from PowerVision+Poly-HRP IHC Detection Systems (Leica, #PY6103). For color development, sections were incubated with DAB reaction product in PowerVision+Poly-HRP IHC Detection Systems (Leica, #PY6103). To ensure the specificity of the staining, liver sections were also stained in parallel with a non-immune rabbit or mouse isotype IgG as a negative control. Finally, the liver sections were counterstained with hematoxylin and cleared with xylene. After mounting, the positive stained liver sections were observed under Nikon Eclipse 80i microscope with 20X and 40X objectives. Staining images were captured and digitalized using a Nikon DS-Fi1 digital camera attached to the Nikon Eclipse 80i microscope.

Immunofluorescent Staining

The 4-μm thick liver tissue sections were prepared, and immunofluorescence of liver tissue sections was performed as described previously (22, 24, 25). After deparaffinization and rehydration, 4-μm thick liver sections were incubated with 10 mmol/L citric acid (pH 6.0) and heated in a microwave at 700 W three times, each heat lasting 2 min, in order to uncover the antigenicity. Nonspecific binding was blocked with 5% normal goat serum in PBST (Vector Laboratories, Burlingame, CA) for 1 h at room temperature. The liver sections were placed in a wet box and incubated with the primary antibody in PBST with 1% BSA at 4°C overnight. The following primary antibodies were used: SREBP-1 (sc#367 K-10, 1:200) and Lipin 1 (CST#14906, 1:100). The sections were then washed three times in PBST and incubated in the secondary antibodies. The SREBP-1 staining was visualized with Alexa Fluor 594 goat anti-rabbit antibody (Invitrogen, red color, 1:500 dilution). Lipin 1 staining was visualized with Fluorescein (FITC)-conjugated donkey anti-rabbit IgG (Jackson ImmunoResearch; #711-096-152, green color, 1:500 dilution). After slides were washed three times in TBST, the cell nuclei were counter-stained with ProLong^{tm} Gold Antifade Mountant with DAPI (Invitrogen, #P36935). The staining signal for SREBP-1 or Lipin-1 in hepatocytes was specific inasmuch as incubation with nonimmuno IgG showed no detectable fluorescence (data not shown). The positive stained liver sections were observed under Nikon Eclipse 80i microscope with 20X and 40X objectives. The fluorescence images were taken under a Nikon Eclipse DS-Qi1MC Digital Camera attached to the Nikon Eclipse 80i microscope.

Immunoblotting Analysis

Immunoblotting analysis was performed as described previously (20, 21) using the following primary antibodies: phospho-Ser2481 mTOR (CST#2974, 1:1000), mTOR (CST#2983, 1:1000); phospho-Thr389 S6K1 (CST#9234, 1:1000), S6K1 (CST#9202, 1:1000); phospho-Ser235/236 S6 (CST#2211, 1:5000), S6 (CST#2212, 1:1500); phospho-Thr37/46 4E-BP1 (CST#9459, 1:2000), 4E-BP1 (CST#9452, 1:2500); DEPTOR (Millipore#ABS222, 1:1000), Rictor (CST#2140, 1:1000), Raptor (CST#2280, 1:500), TSC2 (CST#3990, 1:1000); phospho-Ser473 Akt (CST#9271, 1:1000), Akt (CST#2966, 1:1000); SREBP1 (BD#557036, 1:500), FAS (BD#610963, 1:5000), Lipin 1 (CST#14906, 1:2500), SIRT1 (Upstate Biotechnology #05-707, 1:1000); phospho-Thr202/Tyr204 ERK1/2 (CST#9101, 1:1000), ERK1/2 (SC#94, 1:1000), PPARα (SC#9000, 1:2500), cleaved Caspase-3 (CST#9661, 1:500), PGC-1α (SC#13067, 1:1000), and GAPDH (CST#2118, 1:2000).

Immunoblotting analysis was conducted as described previously (20, 21). Briefly, mouse liver tissues (50-100 mg) were homogenized in a Fisher Scientific™ 125 Homogenizer (Fisher, Cat#08451660) for three cycles of 30 sec in a lysis buffer (20 mM Tris-HCl, pH 8.0; 1% (v/v) Nonidet P-40, 150 mM NaCl, 1 mM EDTA, 1 mM EGTA, 1 mM sodium orthovanadate, 25 mM β-glycerolphosphate, 1 mM dithiothreitol, 1 mM phenylmethylsulfonyl fluoride, 2 μg/ml aprotinin, 2 μg/ml leupeptin, and 1 μg/ml pepstatin). After centrifugation at 14,000 rpm at 4°C for 10 min, protein concentrations were determined using Bio-Rad Protein Dye Reagent. Immunoblotting experiments were performed with 50-100 μg protein of liver lysates in a total 36 μl of protein samples contained 6 μl of 6X loading buffer. After denaturing at 95-100°C for 5 min, equal volumes of samples were separated on 10% SDS-PAGE in a protein electrophoresis running buffer (Bio-Rad, Cat#1610772). Subsequently, protein samples were transferred to a PVDF membrane (Bio-Rad, Cat#1620177) at 100 V at 4°C for 1-2 h in Western blot transfer buffer (Bio-Rad, Cat#1610771). Protein members were washed with Tris-buffered saline with 0.1% Tween-20 (TBST) three times , each wash lasting 5 min, and blocked with 5% non-fat milk in TBST at room temperature for 1 h. The protein membranes were washed and subsequently incubated with a primary antibody at the appropriate dilution in TBST containing 3% BSA at 4°C with gentle agitation overnight. After three washes in TBST, members were incubated with horseradish peroxidase-conjugated secondary antibodies at room temperature for 1 h. Immunoblots were detected by using LumiGLO chemiluminescent detection systems (CST#7003). The intensity of bands were analyzed by scanning densitometry and quantified by NIH Image J software. Phosphorylation levels of mTORC1 signaling were quantified by densitometry, normalized to those of endogenous protein levels, and presented as relative levels to the basal levels of endogenous proteins. For protein expression, specific band intensity was quantified, normalized to those of GAPDH, and presented as a value relative to the control.

RNA Extraction and Quantitative RT-PCR

Quantitative RT-PCR analysis was performed as described previously (20, 21). Approximately 20 mg of liver tissues were homogenized in 1 ml of TRIzol reagent (Invitrogen, Carlsbad, CA, USA) using the 2.8 ceramic beads (MO BIO Laboratories, Cat# 13114-50) and a Bullet Blender homogenizer (Next Advance, USA) at the speed of 4000-6000 RPM for 30 sec with 3-6 times. Total RNA from liver tissues was extracted according to the manufacturer's protocol of the TRIzol reagent. Quantification of total RNA was performed in a Spectramax M5 Microplate Reader (Molecular Devices, Sunnyvale, CA, USA) following the manufacturer's instructions. To synthesize single-stranded cDNA, total RNA (1μg) from each sample was reverse transcribed using High Capacity cDNA Reverse Transcription kit (Applied Biosystems, ABI, USA) according to the manufacturer's instructions. A 20 μl reaction mixurure was made with 10 μl of total RNA, 2 μl of 10X RT buffer, 0.8 μl of 25X dNTP mix (100 mM), 2 μl of 10X RT random primer, 1 μl of MultiScribe™ reverse transcriptase, 1 μl of RNase inhibitor, and 3.2 μl of nuclease-free water. cDNA synthesis was carried out in a Bio-Rad T100 Thermal Cycler (Bio-Rad, USA). The RT-PCR reaction was performed as follows: 25°C for 10 min, 37°C for 120 min, 85°C for 5 min. cDNA samples were stored at -20 °C until use.

The resulting single-stranded cDNA was subjected to real-time PCR with gene-specific primers and SYBR Green PCR master mix using Applied Biosystems 7900HT Fast Real-Time PCR system (ABI, USA) as previously described (3, 9). An amount of 1 μl cDNA was loaded in each reaction to a total volume of 20 μl of the reaction mixture. The specificity of the PCR amplification was confirmed by melting curve analysis and by running the final products on an agarose gel. Quantitative analysis was performed using the comparative ($\Delta\Delta C_T$) method. The mRNA levels of

genes were normalized to those of endogenous GAPDH and expressed as relative levels to the control mice (3, 9). The following primers were used:

Gene name	Forward primers	Reverse primer sequences
SREBP-1c	5'-GGAGCCATGGATTGCACATT-3'	5'-GGCCCGGGAAGTCACTGT-3'
ACC1	5'-TGACAGACTGATCGCAGAGAAAG-3'	5'-TGGAGAGCCCCACACACA-3'
FAS	5'-GCTGCGGAAACTTCAGGAAAT-3'	5'-AGAGACGTGTCACTCCTGGACTT-3'
SCD1	5'-TTCTTCTCTCACGTGGGTTG-3'	5'-CGGGCTTGTAGTACCTCCTC-3'
PPARα	5'-GGGCAGAGCAAGTCATCTTC-3'	5'-CCTCTGGAAGCACTGAGGAC-3'
CPT-1α	5'-CCAGGCTACAGTGGGACATT-3'	5'-GAACTTGCCCATGTCCTTGT-3'
PGC-1α	5'-AAGAGCGCCGTGTGATTTAC-3'	5'-ACGGTGCATTCCTCAATTTC-3'
TNF-α	5'-CGTCAGCCGATTTGCTATCT-3'	5'-CGGACTCCGCAAAGTCTAAG-3'
IL-1β	5'-TTCGTGAATGAGCAGACAGC-3'	5'-GGTTTCTTGTGACCCTGAGC-3'
IL-6	5'-AGTTGCCTTCTTGGGACTGA-3'	5'-TCCACGATTTCCCAGAGAAC-3'
MCP-1	5'-CAGCCAGATGCAGTTAACGC-3'	5'-GCCTACTCATTGGGATCATCTTG-3'
Ly6G	5'-TGCGTTGCTCTGGAGATAGA-3'	5'-CAGAGTAGTGGGGCAGATGG-3'
Mpo	5'-CCCTAGACCTGCTGAAGAG-3'	5'-GTGATGGTGCGATACTTGTC-3'
CD11b	5'-CTGCGAAGATCCTAGTTGTC-3'	5'-GGGACTGTGGTTTGTTGAAG-3'
F4/80	5'-CTTTGGCTATGGGCTTCCAGTC-3'	5'-GCAAGGAGGACAGAGTTTATCGTG-3'
GAPDH	5'-TGCGACTTCAACAGCAACTC-3'	5'-CTTGCTCAGTGTCCTTGCTG-3'

Human Liver Tissue Samples

Normal human liver samples and alcoholic liver disease tissues were obtained from donor livers or recipient livers during liver transplantations from the Liver Tissue Procurement and Distribution System (LTPDS) at University of Minnesota as described previously (1, 26-28). Normal healthy liver samples were provided on the part of donor livers that were not used for transplantation. Alcoholic liver disease was diagnosed by the history of chronic alcohol drinking and liver histology. The liver samples from the patients with malignancies or any other potential risk of liver diseases were excluded. All snap-freezing liver samples were collected in liquid nitrogen and and stored in a -80°C freezer.

Statistical analysis

Data are presented as means ± standard error (S.E.M). Using GraphPad Prism 5.0 software, results were analyzed by one-way ANOVA between multiple groups, when appropriate, and results were analyzed by a two-tailed Student's *t*-test between two groups. $P < 0.05$ was considered statistically significant.

References

1. Bertola A, Park O, Gao B. Chronic plus binge ethanol feeding synergistically induces neutrophil infiltration and liver injury in mice: a critical role for E-selectin. Hepatology 2013;58:1814-1823.

2. Bertola A, Mathews S, Ki SH, Wang H, Gao B. Mouse model of chronic and binge ethanol feeding (the NIAAA model). Nat. Protocols 2013;8:627-637.

3. Li Y, Wong K, Giles A, Jiang J, Lee JW, Adams AC, Kharitonenkov A, et al. Hepatic SIRT1 attenuates hepatic steatosis and controls energy balance in mice by inducing fibroblast growth factor 21. Gastroenterology 2014;146:539-549 e537.

4. Inoki K, Mori H, Wang J, Suzuki T, Hong S, Yoshida S, Blattner SM, et al. mTORC1 activation in podocytes is a critical step in the development of diabetic nephropathy in mice. J Clin Invest 2011;121:2181-2196.

5. Carames B, Hasegawa A, Taniguchi N, Miyaki S, Blanco FJ, Lotz M. Autophagy activation by rapamycin reduces severity of experimental osteoarthritis. Ann Rheum Dis 2012;71:575-581.

6. Sato A, Kasai S, Kobayashi T, Takamatsu Y, Hino O, Ikeda K, Mizuguchi M. Rapamycin reverses impaired social interaction in mouse models of tuberous sclerosis complex. Nat Commun 2012;3:1292.

7. Yin H, Hu M, Zhang R, Shen Z, Flatow L, You M. MicroRNA-217 promotes ethanol-induced fat accumulation in hepatocytes by down-regulating SIRT1. J Biol Chem 2012;287:9817-9826.

8. Bala S, Marcos M, Kodys K, Csak T, Catalano D, Mandrekar P, Szabo G. Up-regulation of microRNA-155 in macrophages contributes to increased tumor necrosis factor {alpha} (TNF{alpha}) production via increased mRNA half-life in alcoholic liver disease. J Biol Chem 2011;286:1436-1444.

9. Li Y, Wong K, Walsh K, Gao B, Zang MW. Retinoic Acid Receptor beta Stimulates Hepatic Induction of Fibroblast Growth Factor 21 to Promote Fatty Acid Oxidation and Control Whole-body Energy Homeostasis in Mice. Journal of Biological Chemistry 2013;288:10490-10504.

10. Chrifi I, Louzao-Martinez L, Brandt M, van Dijk CGM, Burgisser P, Zhu C, Kros JM, et al. CMTM3 (CKLF-Like Marvel Transmembrane Domain 3) Mediates Angiogenesis by Regulating Cell Surface Availability of VE-Cadherin in Endothelial Adherens Junctions. Arterioscler Thromb Vasc Biol 2017;37:1098-1114.

11. Li J, Xu L, Ye J, Li X, Zhang D, Liang D, Xu X, et al. Aberrant dynamin 2-dependent Na(+) /H(+) exchanger-1 trafficking contributes to cardiomyocyte apoptosis. J Cell Mol Med 2013;17:1119-1127.

12. Dierck F, Kuhn C, Rohr C, Hille S, Braune J, Sossalla S, Molt S, et al. The Cardiac Z-Disc Protein CEFIP Regulates Cardiomyocyte Hypertrophy By Modulating Calcineurin Signaling. J Biol Chem 2017.

13. Garanina EE, Mukhamedshina YO, Salafutdinov, II, Kiyasov AP, Lima LM, Reis HJ, Palotas A, et al. Construction of recombinant adenovirus containing picorna-viral 2A-peptide sequence for the co-expression of neuro-protective growth factors in human umbilical cord blood cells. Spinal Cord 2016;54:423-430.

14. Peterson TR, Laplante M, Thoreen CC, Sancak Y, Kang SA, Kuehl WM, Gray NS, et al. DEPTOR Is an mTOR Inhibitor Frequently Overexpressed in Multiple Myeloma Cells and Required for Their Survival. Cell 2009;137:873-886.

15. Li Y, Wong K, Walsh K, Gao B, Zang M. Retinoic acid receptor beta stimulates hepatic induction of fibroblast growth factor 21 to promote fatty acid oxidation and control whole-body energy homeostasis in mice. J Biol Chem 2013;288:10490-10504.

16. Holz MK, Ballif BA, Gygi SP, Blenis J. mTOR and S6K1 mediate assembly of the translation preinitiation complex through dynamic protein interchange and ordered phosphorylation events. Cell 2005;123:569-580.

17. Schalm SS, Blenis J. Identification of a conserved motif required for mTOR signaling. Curr Biol 2002;12:632-639.

18. Zhang J, Gao Z, Yin J, Quon MJ, Ye J. S6K directly phosphorylates IRS-1 on Ser-270 to promote insulin resistance in response to TNF-(alpha) signaling through IKK2. J Biol Chem 2008;283:35375-35382.

19. Zang MW, Zuccollo A, Hou XY, Nagata D, Walsh K, Herscovitz H, Brecher P, et al. AMP-activated protein kinase is required for the lipid-lowering effect of metformin in insulin-resistant human HepG2 cells. Journal of Biological Chemistry 2004;279:47898-47905.

20. Zang MW, Xu SQ, Maitland-Toolan KA, Zuccollo A, Hou XY, Jiang BB, Wierzbicki M, et al. Polyphenols stimulate AMP-activated protein kinase, lower lipids, and inhibit accelerated atherosclerosis in diabetic LDL receptor-deficient mice. Diabetes 2006;55:2180-2191.

21. Hou X, Xu S, Maitland-Toolan KA, Sato K, Jiang B, Ido Y, Lan F, et al. SIRT1 regulates hepatocyte lipid metabolism through activating AMP-activated protein kinase. J.Biol.Chem. 2008;283:20015-20026.

22. Li Y, Xu S, Mihaylova MM, Zheng B, Hou X, Jiang B, Park O, et al. AMPK phosphorylates and inhibits SREBP activity to attenuate hepatic steatosis and atherosclerosis in diet-induced insulin-resistant mice. Cell Metab 2011;13:376-388.

23. Li Y, Xu S, Giles A, Nakamura K, Lee JW, Hou X, Donmez G, et al. Hepatic overexpression of SIRT1 in mice attenuates endoplasmic reticulum stress and insulin resistance in the liver. FASEB J 2011;25:1664-1679.

24. Luo T, Nocon A, Fry J, Sherban A, Rui X, Jiang B, Xu XJ, et al. AMPK Activation by Metformin Suppresses Abnormal Extracellular Matrix Remodeling in Adipose Tissue and Ameliorates Insulin Resistance in Obesity. Diabetes 2016;65:2295-2310.

25. Li Y, Xu S, Jiang B, Cohen RA, Zang M. Activation of sterol regulatory element binding protein and NLRP3 inflammasome in atherosclerotic lesion development in diabetic pigs. PLoS One 2013;8:e67532.

26. Mukhopadhyay P, Horvath B, Rajesh M, Varga ZV, Gariani K, Ryu D, Cao Z, et al. PARP inhibition protects against alcoholic and non-alcoholic steatohepatitis. J Hepatol 2017;66:589-600.

27. Calvisi DF, Ladu S, Gorden A, Farina M, Lee JS, Conner EA, Schroeder I, et al. Mechanistic and prognostic significance of aberrant methylation in the molecular pathogenesis of human hepatocellular carcinoma. J Clin Invest 2007;117:2713-2722.

28. Cai Y, Jogasuria A, Yin H, Xu MJ, Hu X, Wang J, Kim C, et al. The Detrimental Role Played by Lipocalin-2 in Alcoholic Fatty Liver in Mice. Am J Pathol 2016;186:2417-2428.

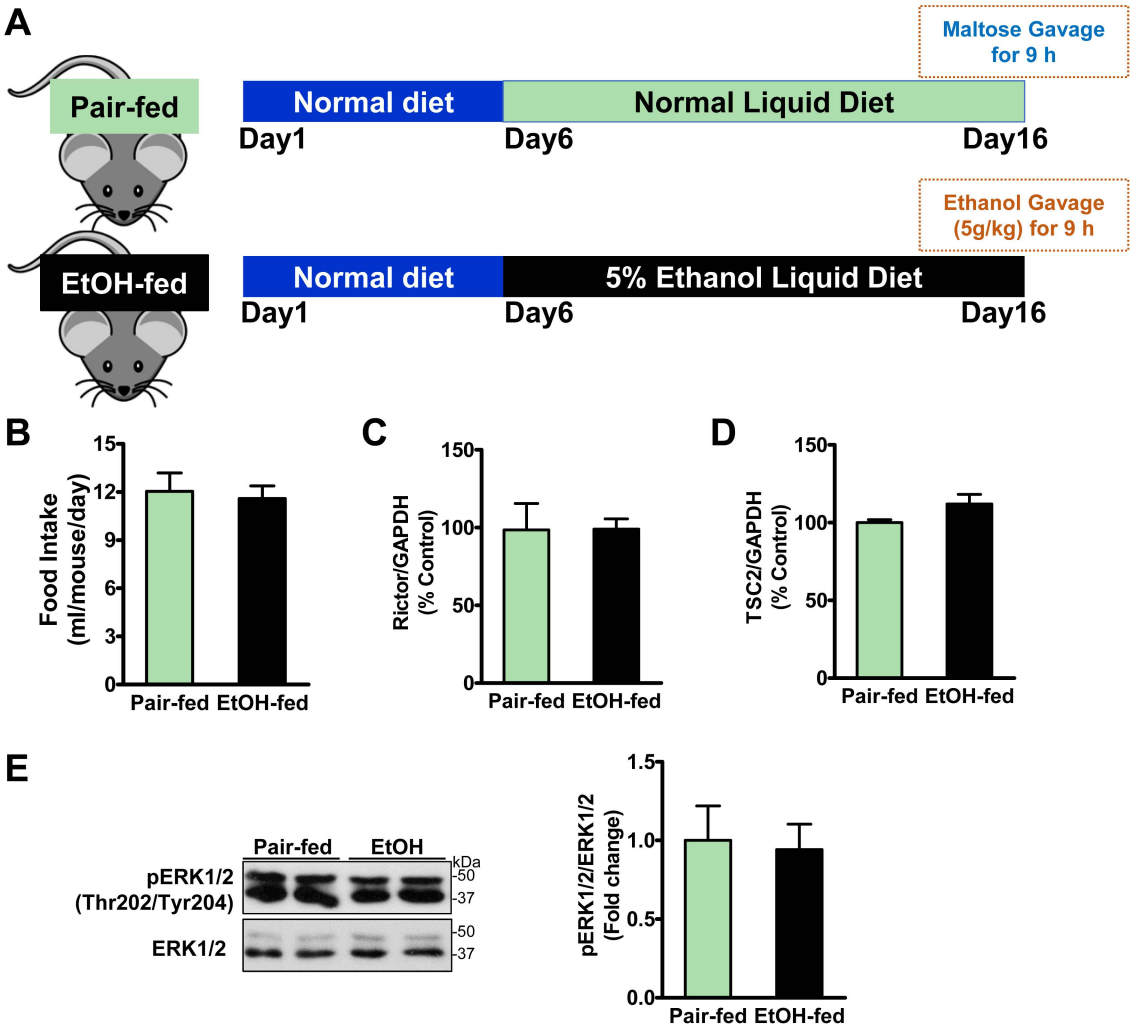

Fig. S1. The effect of chronic-plus-binge ethanol feeding on key regulators of mTORC1 and mTORC2 in mice.

A. Schematic image of a mouse model of chronic-plus-binge ethanol feeding, referred to as Bin Gao's Chronic-Binge model. C57/BL6 mice were fed an isocaloric control diet (pair-fed) or Lieber-DeCarli liquid ethanol diet (EtOH-fed) for 10 days, followed by a single gavage of maltose or ethanol (5g/kg), respectively. Mice were euthanized at 9 h after gavage.

B. The effect of chronic-plus-binge ethanol feeding on food intake in mice.

C-D. The densitometric quantification of protein levels of Rictor, a major component of mTORC2, and TSC2, an negative regulator of mTORC1, is assessed by Image J, normalized to GAPDH levels, and presented as relative levels to the control mice.

E. Hepatic phosphorylation of ERK1/2, the upstream kinase of the TSC complex, is not significantly altered by chronic-plus-binge ethanol feeding in mice.

The data are presented as mean ± SEM, n =6-8 (pair-fed); n = 7-8 (EtOH-fed).

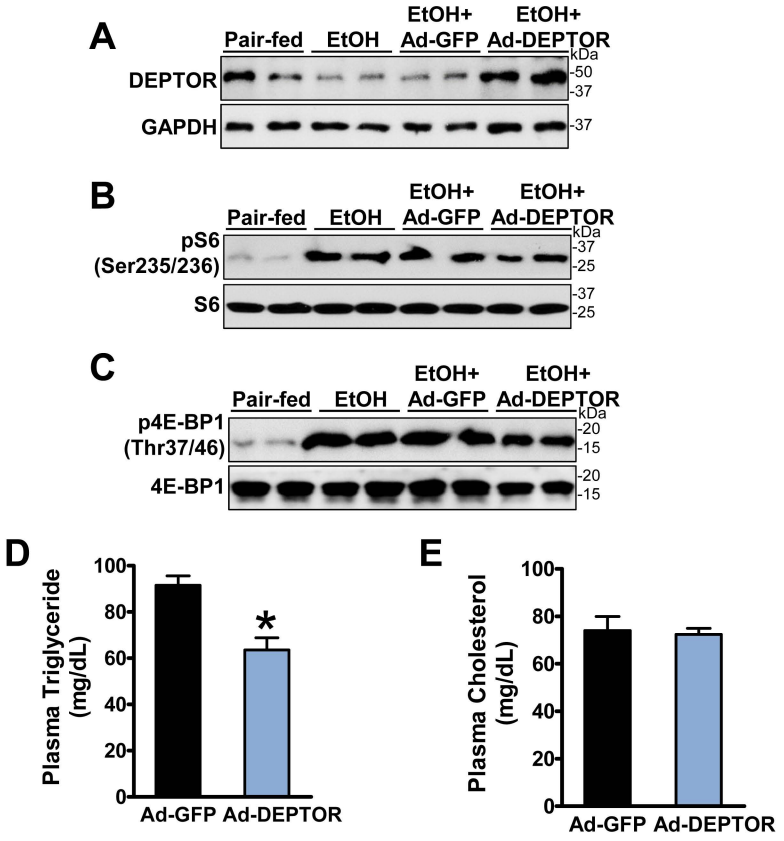

Fig. S2. Adenoviral overexpression of DEPTOR in the liver restores DEPTOR function, reduces mTORC1 signaling, and modulates plasma lipid profile in chronic-binge ethanol-fed mice.

Adenoviruses encoding DEPTOR (Ad-DEPTOR) or GFP (Ad-GFP) (1×10^9 to 5×10^9 pfu) were delivered into the livers of C57BL/6 mice through tail vein injection, and the animals were fed an ethanol diet for 10 days, followed by a single binge ethanol feeding at the end of experiments. Mice were euthanized 9 h after gavage.

A-C. The effect of hepatic overexpression of DEPTOR on mTORC1 signaling in chronic-binge ethanol-fed mice.

D-E. Hepatic overexpression of DEPTOR lowers plasma triglyceride levels but does not affect plasma cholesterol levels in chronic-binge ethanol-fed mice.

The data are presented as mean ± SEM, n =6-8 each group. *P < 0.05 vs. ethanol-fed mice with Ad-GFP injection.

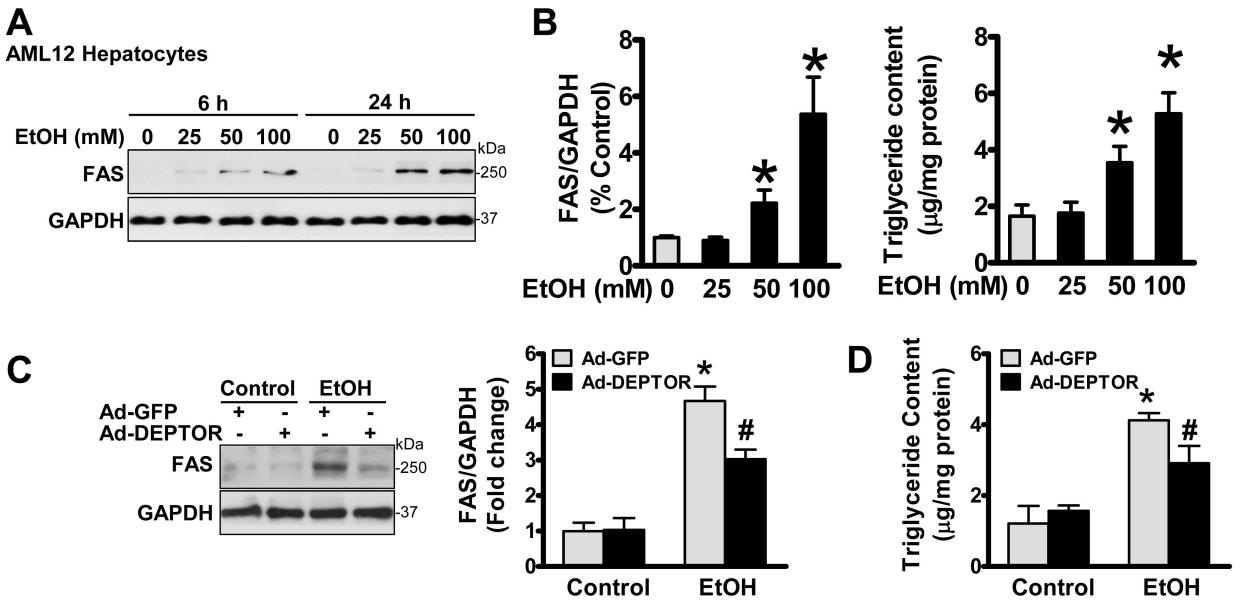

Fig. S3. Overexpression of DEPTOR inhibits FAS induction and lowers triglyceride accumulation in AML 12 mouse hepatocytes exposed to ethanol.

A. Treatment with increasing concentrations of ethanol (25-100 mM) for 6 h or 24 h leads to increased expression of FAS in a dose- and time-dependent manner.

B. Treatment with increasing concentrations of ethanol (25-100 mM) for 24 h resulted in the induction of FAS expression and elevation of triglyceride content in a dose-dependent manner in AML 12 hepatocytes.

AML 12 cells were maintained in DMEM/F12 medium containing 2% FBS overnight prior to the experiments and incubated with increasing concentrations (25-100 mM) of ethanol as indicated times. *P < 0.05 vs. control cells (mean ± SEM, n = 3-4).

C. Overexpression of DEPTOR inhibits the upregulation of FAS in AML 12 cells exposed to ethanol. AML 12 cells were infected with adenoviruses encoding either GFP (Ad-GFP) or DEPTOR (Ad-GFP), maintained in DMEM/F12 medium containing 2% FBS overnight, and incubated with ethanol (100 mM) for an additional 24 h. No detectable difference in endogenous FAS was observed in cells expressing GFP or DEPTOR under normal conditions.

D. Intracellular triglyceride content is elevated by ethanol exposure in AML 12 hepatocytes and the triglyceride overproduction is largely attenuated by DEPTOR overexpression. Notably, no significant alterations in triglyceride content were evident in AML-12 hepatocytes expressing GFP or DEPTOR under normal conditions.

*P< 0.05 *vs.* untreatment in cells expressing control GFP; #P< 0.05 *vs* ethanol treatment in cells expressing control GFP (mean ± SEM, n = 3-4).

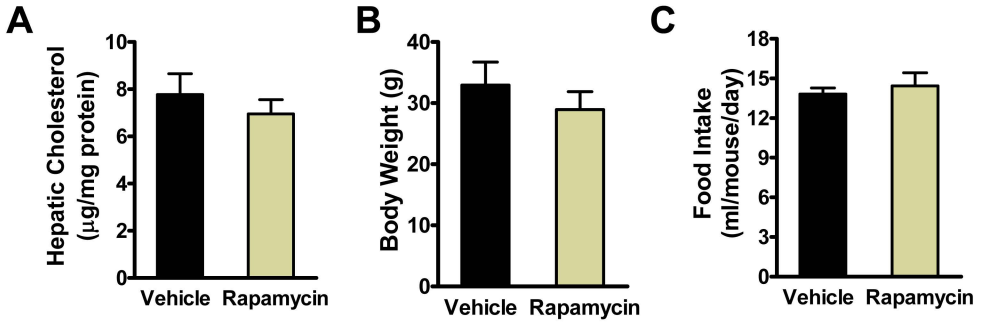

Fig. S4. The effect of rapamycin administration on hepatic cholesterol, body weight, and food intake in chronic-binge ethanol-fed mice. Mice fed the ethanol diet were given intraperitoneal injections daily with either vehicle or a single dose of rapamycin. After administration with rapamycin (1 mg/kg/day, i.p.) for 10 days, mice were gavaged with a single dose of ethanol (5 g/kg) and then sacrificed 9 hours after the gavage.

A. Hepatic cholesterol content was measured and expressed as μg of lipid/mg of protein.

B-C. No significant difference in body weight and food uptake between two groups of the mice.

The data are presented as mean ± SEM, n = 6-8 each group.

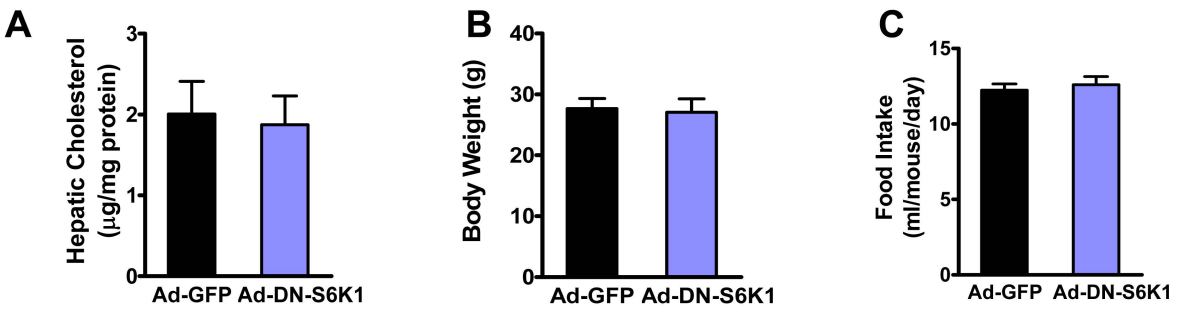

Fig. S5. The effect of hepatic overexpression of DN-S6K1 on hepatic cholesterol, body weight, and food intake in chronic-binge ethanol-fed mice. Adenoviruses encoding DN-S6K1 (Ad-DN-S6K1) or GFP (Ad-GFP) (1×10^9 to 5×10^9 pfu) were delivered into the livers of C57BL/6 mice through tail vein injection. The animals were fed an ethanol diet for 10 days, followed by a single binge ethanol feeding at the end of experiments. Mice were euthanized 9 h after gavage.
The data are presented as mean ± SEM, n = 6-8 each group.

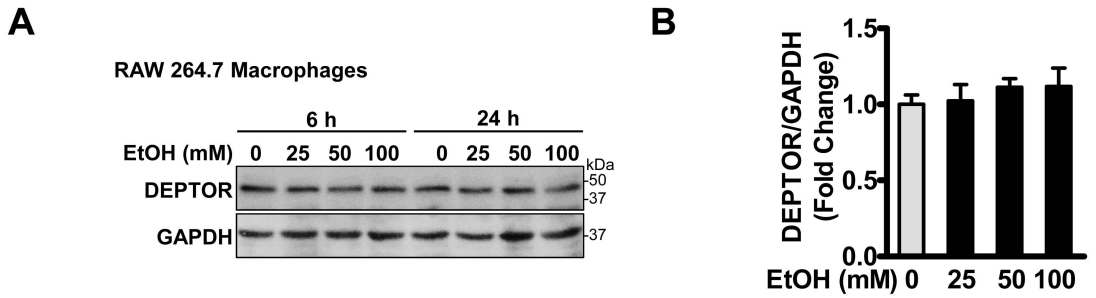

Fig. S6. The effect of ethanol treatment on DEPTOR in RAW 264.7 mouse macrophages.
A. RAW264.7 cells were maintained in DMEM medium containing 2% FBS overnight and incubated with increasing concentrations (25-100 mM) of ethanol for indicated times.
B. Treatment with increasing concentrations of ethanol (25-100 mM) for 24 h does not significantly affect protein levels of DEPTOR in RAW 264.7 cells.
The data are presented as mean ± SEM, n = 3.

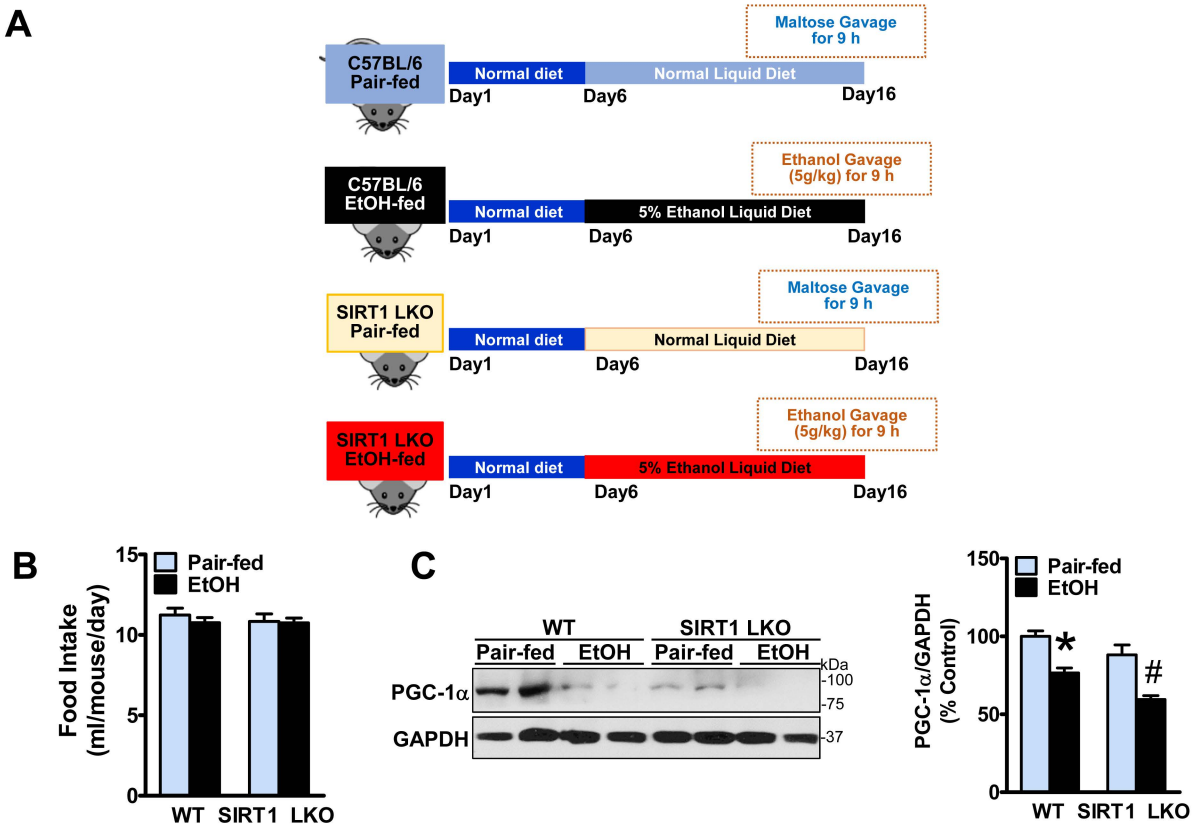

Fig. S7. SIRT1 LKO mice are more susceptible to developing alcoholic fatty liver.

A. Schematic image of WT and SIRT1 LKO mice with a pair-fed diet and chronic-plus-binge ethanol feeding. Mice were fed an isocaloric control diet (pair-fed) or Lieber-DeCarli liquid ethanol diet (EtOH-fed) for 10 days, followed by a single gavage of maltose or ethanol (5g/kg), respectively. Mice were euthanized at 9 h after gavage.

B. The effect of chronic-binge ethanol feeding on food intake in both WT and SIRT1 LKO mice.

C. Chronic-binge ethanol feeding significantly decreases expression of PGC-1α in WT mice and the inhibition is more pronounced in ethanol-fed SIRT1 LKO mice.

The data are presented as mean ± SEM, n = 4-8 each group. *P< 0.05, vs. pair-fed WT mice; $^{\#}$P < 0.05, vs. ethanol-fed WT mice.